

# Chapter 2

---

**Preparation methods and  
characterization techniques**

## **2. Nanoparticle preparation methods:**

Nanoparticles are generally synthesized through two different techniques, top-down and bottom-up. Bottom-up techniques are associated with molecular scale electronics where molecules are known with precise electronic function. Nature implements bottom-up approach for the evolution of cells and living beings, whereas chemistry and biology help in their controlled assemble. The bottom-up fabrication techniques include sol-gel synthesis, hydrothermal growth, precipitation method, chemical vapor deposition, physical vapor synthesis and pulsed-laser synthesis etc. In top-down approach nanostructures are fabricated of microstructures, whereas the bottom-up method is related to self-assembly of atoms or molecules into nanostructures. Some top-down methods are ball milling, photolithography and ion beam lithography.

### **2.1. Synthesis methods of ZnO:**

There has been a durable interest in development of growth techniques, enabling the assembly of ZnO nanostructures with tunable size and shape, for applications in diverse fields. Size and shape of ZnO nanoparticles sturdily depends on the environment of fabrication method. A minute change in growth environment significantly affects the size and property of the compounds. Other important aspects considered while selecting the synthesis method pertains to high product yield, simple equipment necessities and low manufacture cost. Some of the fabrication methods of the nanoparticles of ZnO are listed below with their main functions and drawbacks. The pros and cons of these methods are tabulated in last part of this section.

#### **2.1.1. Solution combustion method:**

Solution combustion method is emerged as a facile technique for the synthesis of ceramics, alloys and nanomaterials [167, 168]. Combustion synthesis approach is designed

on the basis of the thermo-chemical concept used in the field of propellants and explosives. This approach is included with heating and evaporation of the metal nitrate solutions with an organic compound such as glycine, urea, dextrose, citric acid etc. During the process highly exothermic reaction takes place due to self-firing. The strong heat yields voluminous powder production. Combustion method has been adopted by many research teams for the fabrication of ZnO based nanostructures [169-171]. The high reaction temperature combined with complex reaction mechanism and the high price per yield are some of the drawbacks of the solution combustion synthesis.

### **2.1.2. Hydrothermal method:**

In hydrothermal method the chemical reactions of the precursors proceed at ambient temperature and pressure in a sealed autoclave. The temperature of the precursors materials are gradually increased from 100 to 300 °C during the time of synthesis [172]. Several literature have conveyed that the structural morphology of ZnO nanocrystal and its ultimate size can be controlled with handling parameters such as reaction time, temperature and the nature of surfactant [173, 174]. In this growth technique, the reaction mixture is slowly heated to the reaction temperature and then cooled to room temperature. Firstly, the nucleation of crystal ZnO form and then grow to various sizes and morphologies based on reaction conditions. The particle size achieved by this method remains in the range of 30-70 nm. Yet, some limitations of hydrothermal process are related to the complexity in controlling the growth process and relatively large time duration required for the yield of the nanoparticles.

### **2.1.3. Chemical Vapor Deposition:**

CVD technique is associated with gaseous precursors and gaseous reaction at the substrate surface, leading to the deposition of a nanostructured film. Vacuum is usually not

needed for CVD growth technique. In this process a chemical reaction takes place between volatile compound and other gases to generate a non-volatile solid that is deposited on a substrate. High temperature CVD approach is convenient to manufacture thin films, required for application in solid state devices, nuclear reactor components, coating for rocket engine components and high quality metal oxide semiconductor (MOS) transistors. Researchers use various types of CVD methods like low pressure CVD, plasma-enhanced CVD and laser enhanced CVD. However, the CVD technique is more expensive and the process needs very high temperature.

#### **2.1.4. Physical Vapor Deposition:**

Mainly the solid and molten sources have been used in PVD technique. In this physical process the source atoms in gas phase suffer collision, compound formation and then deposition on the substrate. First a solid precursor material is chosen and then vaporized. The reaction occurs between the base materials, in the form of a vapour resulting in the creation of clusters/ions. The vapour and gas mixture is cooled down to produce nanocrystal. The epitaxial growth roots, specifically, molecular beam epitaxy (MBE) and metal-organic vapor phase epitaxy (MOVPE) are usually applied for the growth of thin film heterostructures, superlattices and quantum wells. Pulsed laser deposition (PLD) is another vital PVD technique. The disadvantage of PVD techniques is that it needs too much expensive complicated vacuum equipment and results in little yield though in the pure desired form.

#### **2.1.5. Spray Pyrolysis:**

In spray pyrolysis method ZnO nanoparticles is prepared by making droplets on a substrate through atomization of precursor solutions and the reaction occur at high temperature to form the end product [175]. Also ZnO nanoparticles were prepared through

flame spray pyrolysis of zinc acrylate-methanol-acetic acid solution [176]. Again the selection of the precursor materials is vital since morphology and structure of prepared yields is significantly affected by the chemical nature of the precursor material. The particle size distribution realized by this method is 1-2  $\mu\text{m}$ . Spray pyrolysis technique has some drawbacks like low yield, probable oxidation of sulphides when the process is in air atmosphere.

#### **2.1.6. Micro-emulsion method:**

Another technique to prepare ZnO nanoparticles is micro-emulsion technique which offers controllable size and morphology of the ZnO powders in the nanometer range. Depending on thermal stability and dispersion properties of two dissimilar liquids, the process can be categorized as macro, mini or micro-emulsion. The observed droplet size for macro, mini and micro-emulsion are 2-20, 0.1-0.3 and  $<0.1 \mu\text{m}$  respectively. Micro-emulsion is more thermodynamically stable than the macro-emulsions because the assimilation of phase occurs in a very short time. Also, the mechanical stirring is needed for macro-emulsions to attain temporary stability [177]. Micro-emulsions are clear or translucent, while macro-emulsions are cloudy. The limitations of micro-emulsion process are that it necessitates large concentration of surfactant and co-surfactant for stabilizing the droplets of micro-emulsion and it has low stabilizing capability for substances with high-melting point used in the system.

#### **2.1.7. Sol-gel method:**

The transformation of liquid solute phase to a solid gel type network is achieved commonly by sol-gel method. It includes physico-chemical reactions comprising hydrolysis, condensation, drying and densification [178]. A sol is defined as spreading of colloidal particles and/or polymers with a stable of solvent and gel comprises isotropic, homogeneous,

continuous network in three dimensional. Usually Van-der Waals forces or hydrogen bonds are active between the sol particles. Gel may be designed with linking network of polymer chains. The interactions involve in almost all the gel systems being covalent in nature. The gel process is primarily irreversible. If the gel is dried by evaporation, then shrinkage on the basis of the capillary results in the collapse of the gel network, and the formation of a xerogel. When drying is executed with the specific conditions, the structure of the polymer network may be remained same and a large number of pores within the gel may be molded. This is known as an aerogel and this type of gel has very lower density. For the creation of single phase, the aerogel is calcined at an appropriate temperature. Several morphological nanosized ZnO can be fabricated through sol-gel technique. Ba-Abbad et al. studied preparation of spherical shaped ZnO powders by sol-gel method and the effect of molar composition of the precursor materials, pH of the solvent and the preparation temperature on the nanostructures of ZnO [179]. For fabrication of ZnO nanostructures sol gel method is quite attractive because of its simplicity, low cost, reliability and comparatively mild conditions of synthesis compared to other discussed methods. While in earlier techniques the particle size remains in the range of 30 nm-2  $\mu$ m, in sol-gel method the particle size easily can be made in the range of 10-20 nm. In this present work, iron doped ZnO samples with particle size of nearly 17.5 nm were synthesized through the sol-gel route.

#### **2.1.8. Chemical precipitation method:**

Chemical precipitation method is a very easy, inexpensive and reliable fabrication technique at ambient temperature. Heat consumption and time duration per yield is also very small in this technique. This technique is advantageous to acquire highly pure and highly crystalline yields and also expedient to monitor the particle size and structural morphology by controlling the base materials, reaction atmosphere (temperature, time etc.). Aqueous precipitation method is an economically favorable method for large scale production of pure

ZnO nanoparticles. Precipitation method is usually monitored by the pH of solution, temperature, time, concentration of precursor reagents [161, 180]. Hong et al. described a controlled precipitation method using zinc acetate [ $\text{Zn}(\text{CH}_3\text{CO}_2)_2$ ] and ammonium carbonate [ $(\text{NH}_4)_2\text{CO}_3$ ] as precursor and precipitating agent [181]. In that literature ZnO nanoparticles with the diameter of 30 nm was obtained and the agglomeration of the particles were restrained by the heterogeneous azeotropic distillation of the precursor material. The shape and size controlled precipitation technique was also reported by Li et al. [182]. Different shapes like rice grains, nuts, flowers, tubes and rods were formed using zinc nitrate hexahydrate and NaOH in the environment of sodium dodecyl sulphate and triethanolamine as manifest cationic surfactants. The nature of solvent for preparation has also an influence on morphology of ZnO nanostructures. Here Ni, Co, Mg and Nd-incorporated ZnO nanopowders have been prepared within the range of 20-30 nm particle size through chemical precipitation method using hydroxylate type precursors. A schematic representation of chemical precipitation method is shown in figure 2.1.

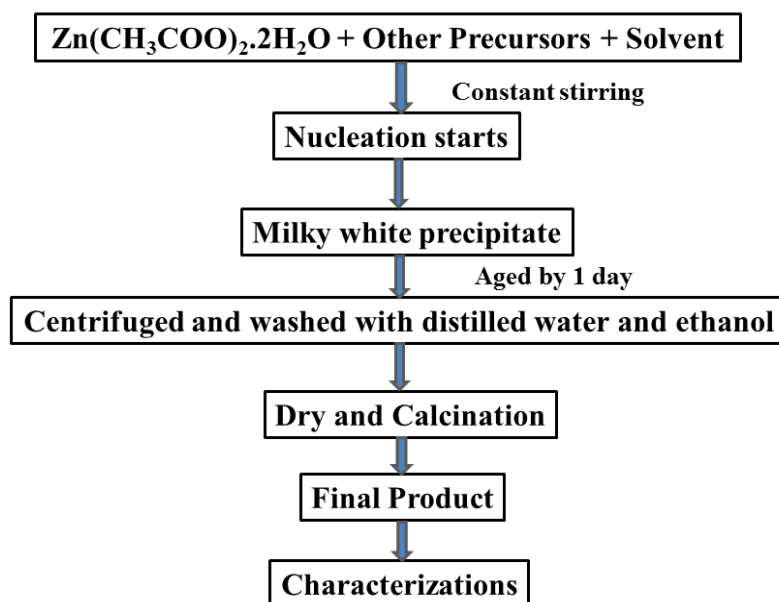


**Fig. 2.1.** Chemical precipitation method.

• **Pros and Cons of various synthesis methods in tabular form:**

<b>Synthesis techniques</b>	<b>Pros</b>	<b>Cons</b>	<b>Ref.</b>
<b>Solution combustion method</b>	A chemical process involving self-sustained exothermic reactions in an aqueous/solvent based medium. Generally employed for nano-scale synthesis of oxides, alloys etc. Yields voluminous powder.	For reaction to proceed at molecular level parameters such as fuel type, solvent medium, pH, metal cation precursors and other reaction conditions are required to be controlled.	[169-171]
<b>Hydrothermal method</b>	Based on the solubility of the reactants in hot water under high pressure. Suitable for the growth of large good-quality crystals. The crystal is grown in a steel pressure vessel called an autoclave. Have the ability to control the size and shape of the end product.	The process requires expensive autoclaves and there is no provision for observing the growth at any time before completion.	[172-174]
<b>Chemical Vapor Deposition</b>	A process in which volatile vapors of the desired material is made to react over the surface of a substrate. The vapor reacts with the substrate to form the desired compound mainly in the form of thin films. The film developed is of high quality and are being used in solid state devices.	Need expensive and sophisticated instrumentation. Generally operated at high temperature and low pressure.	[156]
<b>Physical Vapor Deposition</b>	Involves the deposition of vapor of the desired material on an electrically conducting material. The process involves three phases sputtering, evaporation and ion	Higher costs, expensive and complex machines that requires skilled technician to handle. Carried out in high vacuum conditions ( $10^{-6}$	[4]

	plating. Usually applied for the growth of thin film heterostructures, superlattices and quantum wells.	torr). Very slow rate of deposition.	
<b>Spray Pyrolysis</b>	Involves the deposition of thin film of a compound by spraying up the solution of the reagents on a heated surface, where they react to form the desired compound. Does not need high quality targets, low cost method. The particle size distribution realized by this method is 1-2 $\mu\text{m}$ .	Precaution should be taken such that the other byproducts in the chemical reaction should be volatile. Complications in defining the growth temperature and probable oxidation of sulphides in air atmosphere. Low yield.	[175, 176]
<b>Micro-emulsion method</b>	Generally require a polar liquid (usually water), a nonpolar phase (oil) and a surfactant which forms the inter-phase film. Easy to synthesize without any energy input. Offers controllable size and morphology of the ZnO powders in the nanometer range.	Require large concentration of surfactant and co-surfactant for stabilizing the droplets of micro-emulsion. Require temperature and pH control.	[177]
<b>Sol-gel method</b>	In the method solutions of reactive precursors like alkoxides or metal salts are used. The advantages are the simplicity, low cost, reliable and comparatively mild conditions of synthesis. The particle size is in the range of 10-20 nm.	Longer time required to achieve the nanoparticles. Care should be taken to minimize residual hydroxyl and/ or carbon groups.	[178, 179]
<b>Chemical precipitation method</b>	Very easy, inexpensive and reliable fabrication technique at ambient temperature. Small heat and time consumption. The yield particle diameter is around 30 nm.	Relatively higher chemical consumption. Require physiochemical monitoring.	[180-182]

## 2.2. Characterization techniques:

This portion relies on an outline of the investigating methods those were applied to study the different properties of nanostructured pure and doped ZnO powders.

### 2.2.1. X-ray diffraction:

X-ray diffraction was applied to determine the structural properties and the crystalline phase of samples. The XRD data analyses provide us the knowledge about the crystallinity of the material, phase of the samples, lattice parameters, average crystalline diameter and interplanar distance. When an X-ray with selected wavelength strikes an atom, the scattering will be occurred in all directions. If a periodic arrangement of atoms is encountered by X-ray, the beams scattered by the atoms will strengthen in particular directions and terminate in others. When the scattered beams from a specified group of planes reach at the detector in same phase, they interfere constructively. The constructive interference of waves is achieved in a direction with deviation angle  $2\theta$  following Bragg's law (exhibited in figure 2.2).

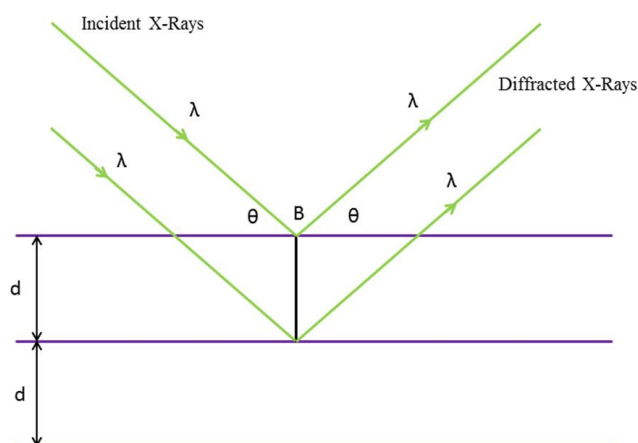


**Fig. 2.2.** A presentation of Bragg's diffraction of X-ray beam from atomic planes.

Constructive interference of the waves from consecutive planes occur when the path difference between two waves diffracted from two parallel planes is an integral multiple of wavelength  $\lambda$ , i.e.,  $2d\sin\theta = n\lambda$  where  $d$  is the interplanar spacing and  $\theta$  is grazing angle of the

incident X-ray with the parallel plane. A representation of XRD experimental set up is displayed in figure 2.3.



**Fig. 2.3.** Representation of XRD experimental set-up.

The X-ray characterization has been done using a Rigaku Mini Flex-600 with  $\text{CuK}_\alpha$  ( $\lambda = 1.5418 \text{ \AA}$ ) radiation and the angle of deviation of the scattered wave  $2\theta$  scanned between  $20^\circ$  and  $80^\circ$ . The shift in peak position with the incorporation of doping material in the host and also with the change in dopant concentration offers valuable information. Every material is characterized with a significant diffraction pattern. The crystal structure determination of the unknown materials is being obtained by analysis of the XRD data by appropriate software like POWD and also by comparing with known database. The average crystalline diameter of the particles can be calculated using the Scherrer equation  $D = k\lambda/\beta\cos\theta$  where  $D$  is average crystalline diameter,  $k$  is a constant equal to 0.9,  $\lambda$  is the wavelength of X-ray,  $\theta$  is the Bragg's angle and  $\beta$  is the FWHM of the diffraction peak at the Bragg angle  $\theta$ .

### **2.2.2. Transmission Electron Microscopy:**

The structure and morphology of the samples have been investigated by transmission electron microscopy (TEM). The working principle of TEM is similar to that of a slide projector with electrons instead of light. A beam of high energy electrons is emitted from an electron gun. This emitted electron beam strikes the sample and a portion of this beam is transmitted through the sample. The electrons are interacted with the atoms of the sample. This interaction can be used to determine internal structure, grain boundaries, chemical

analysis etc. These transmitted electrons are allowed for focusing and amplification. The contrast of image is improved by blocking out high-angle diffracted electron and the image is conceded through imaging device like a phosphor screen. The entire arrangement is conducted under high vacuum condition. The TEM resolution stands at less than 1 nm. Samples for the purpose of TEM analysis are prepared in the following process. Very small amount of powder sample is dispersed in a proper solvent (like acetone, distilled water or ethanol which does not react with the sample) through sonication by an ultrasonicator for half an hour or more depending on the type of the sample. A drop of arranged solution is then placed on a carbon coated copper grid which acts as a support for the sample under investigation, without disturbing the sample properties. The grid with sample is dried well and then used for capturing the images. High resolution TEM (HRTEM) is used for lattice spacing calculation. In the present research work, the FETEM-Jeol 2010 has been used for the investigation of particle size, lattice spacing and constituent elements of the nanopowders. Different magnification scales has been arranged to evaluate the samples. The different size and length related to the images has been analyzed using Image J software.

### **2.2.3. Energy Dispersive X-ray analysis:**

Chemical composition of the samples can be investigated using energy dispersive X-ray (EDX) analysis skill endorsed with a TEM. When an incident electron beam strikes the sample, secondary electron (SEs) and back-scattered electron (BSEs) are radiated from the sample. When the incident beam bounces through the specimen generating secondary electrons, it creates holes in the electron shells where the SEs used to be. In some cases due to transfer of energy from the incident beam the electrons from the core states are being excited to a higher orbit leaving behind a hole. The holes so created in the inner shells results in an unstable condition and subsequently the electrons from higher shells make transitions into the inner shells to restore stability to the atom and thus emit an X-ray whose energy is

the difference in energy of the two shells. The emitted X-ray of specific energy and wavelength is the characteristic of both the elements (atomic number) and the shells between which the transition is really effected. Fundamentally, each element possesses a characteristic X-ray line that helps to recognize the elements in a sample. The emitted X-rays come from a depth corresponding to the forming level SEs. In consequence with the sample density and accelerating voltage of the incident beam, this generally arises from a depth around 0.2-0.5 micron. By calculating the area under the peak of each identified element and the accelerating voltage of the beam it is possible in EDX analysis to determine the weight or atomic percent of constituting elements. However there is a point of caution on the EDX analysis which does not give an exact count of the elements of the first and second period in the periodic table. The X-ray emitted from the elements in the first and second period of the periodic table are really soft X-rays with lower energy and higher wavelength and a fraction of which gets absorbed in the sample resulting in lower count.

#### **2.2.4. Infrared spectroscopy:**

Infrared (IR) spectroscopy is an important device to investigate the structure for the low dimensional molecules in polymer chemistry, organic chemistry, forensic science and other related areas. It directly provides the vibrational frequencies corresponding to the atomic bonding in molecules which depend on the atomic masses with vibrational motion, the bond strength and angles which are parameters of the molecular structure. IR spectrum is usually acquired through the incidence of infrared radiation over a specimen and measuring the fraction of the incident radiation absorbed at a particular energy. FTIR delivers the details of whole IR spectrum and then transforms the scanning data into absorbance/transmitted spectra vs. wavenumber. Figure 2.4 exhibits a schematic view of FTIR spectrophotometer. The working principle of FTIR is similar to that of Michelson interferometer (figure 2.5).

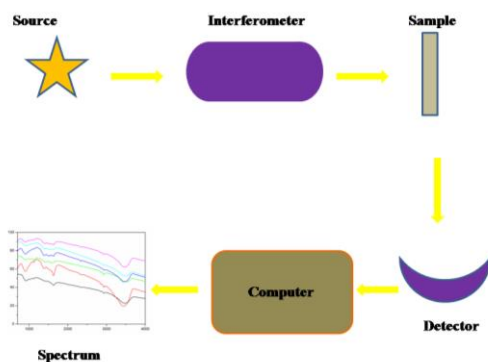


**Fig. 2.4.** A schematic view of FTIR spectrophotometer.

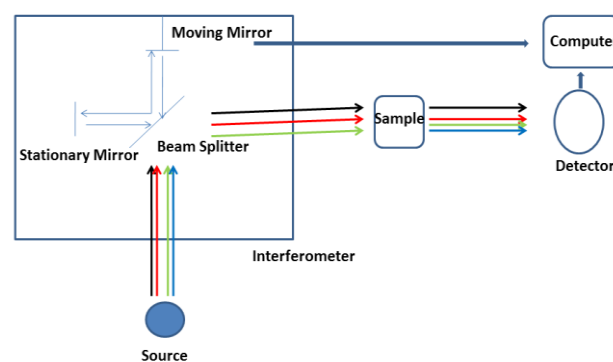


**Fig. 2.5.** Working principle of FTIR spectrophotometer.

Using an interferometer, the source energy is directed onto the sample. When the light incident on the beam splitter, the beam of light splits into right angles in two directions. One beam drives towards a stationary mirror then reflected back to the splitter while other drives to a moving mirror. When the two beams superpose, constructive/destructive interference occur based on the path difference between the two beams. In an interferogram the combined beam goes through the sample. The sample absorbs lights of various wavelengths and the lights of specific wavelengths are subtracted from the interferogram. Now the energy vs. time for all wavelengths is recorded simultaneously by the detector. Fourier transform offers the scope to transform intensity versus time to intensity versus frequency spectrum. In the present research work, data was recorded using BX-II spectrophotometer in the range  $400\text{-}4000\text{ cm}^{-1}$  to determine the bond and the bond angle. Gaussian software was taken to fit the various peaks at the separate positions. The FTIR study has been done in open air condition.

### 2.2.5. Optical characterizations:

Absorption spectroscopy is just opposite to that of a fluorescence spectroscopy. A fluorescence spectrum relies on the emission during transition from the state of excitation to the lower energy state, while the absorption spectrum records the transitions from the lower

energy state to the higher excited state. The optical characterization equipment used for present research works are deliberated in the following:

### **UV-Vis spectroscopy:**

UV-Visible spectroscopy is commonly recognized as absorption spectroscopy and has been operated within the ultraviolet and visible spectral region. This is the expanse of electromagnetic spectrum where molecules are bound to experience an electronic transition. If an incident photon strikes a molecule in its lower energy state, the molecule suffer a transition by absorbing the energy of the photon to an excited state. The excitation occurs only when the incident photon energy becomes equal to the energy separation between the lower energy state and the excited state. The transmitted light decreases through the mechanism of the absorption process according to Beer-Lambert law with the characteristics of the material. Figure 2.6 represents a schematic setup for absorption/transmission study using the Beer-Lambert law. The law may be expressed in terms of absorption coefficient ( $A$ ) in the logarithmic scale of relative decrement of intensity:  $A = -\log_{10}(I_0/I)$  where  $I_0$  and  $I$  are light intensities before and after the specimen. Usually the absorption spectra have been recorded between wavelength region of 200-800 nm. If all transitions take place between the first excited state and the lowest vibrational energy levels of the ground state, then a discrete peak is observed in absorption spectrum. Again the transition between many vibrational levels takes place during transition from an electronic level to the other. The optical absorbance spectra have been studied by using Parkin Elmer Lambda-35 UV-Vis spectrometer in range of wavelength between 200-800 nm. A schematic representation of this set-up is displayed in figure 2.7.

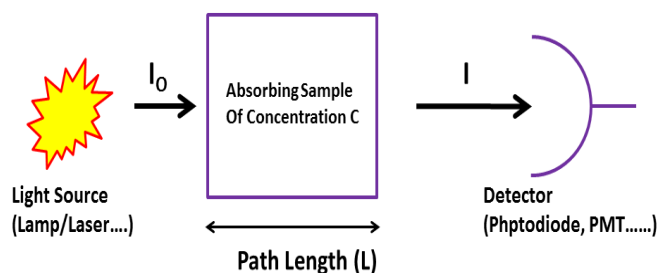


**Fig. 2.6.** Schematic set-up for absorption measurements.



**Fig. 2.7.** Schematic set-up of Lambda-35 double beam UV/Vis spectrophotometer.

### Photoluminescence (PL) spectroscopy:

For photoluminescence (PL) spectroscopy, white light possessing a broad range of wavelengths in the electromagnetic spectrum is beamed on a sample for excitation. Generally xenon lamp whose wavelength lies in the region ranging from ultraviolet through the visible to the infrared is being employed for the purpose. A light of particular wavelength for excitation is perceived by an excitation monochromator and then a slit is used to monitor the intensity of photons striking the sample. The light emission from the sample is collected by the detector using a secondary emission monochromator which is located normal to the incoming beam and then connected to a computer for recording the emission data. Fluorescence is the main features of PL spectroscopy and is comprised with three-stage process of the electron shells of various molecules. The three processes engaged with fluorescence are excitation, non-radiative transitions and fluorescence emission.

PL characterization has been used to analyze various parameters of the materials such as band gap, defect and impurity level etc.

- (i) Detection of band gap: Most of the emissions in PL spectra of semiconductors arise due to transition between different states of the conduction and valence bands and in effect determine the optical band gap of the specimen. Band gap energy measurement is mainly fruitful when working with newly prepared semiconductor compounds.

- (ii) Recognition of impurity energy levels and defect states: The PL energy accredited with various defects and impurity levels can be recognized with the PL intensity which can be governed to detect their amount in composites.
- (iii) Recombination mechanism: Recombination is related with both radiative and nonradiative mechanism. The recombination mechanism provides the PL intensity and its direct dependence on the photo-excitation and temperature.

The schematic of PL (fluorescence) set-up is presented in figure 2.8. Perkin Elmer LS 55 fluorescence spectrometer has been used to investigate the luminescence properties of the compounds and the samples were excited with Xe Laser of wavelength 325 nm.



**Fig. 2.8.** The schematic of fluorescence experimental set-up.

### **Photocatalytic activity:**

The photocatalytic degradation of organic and inorganic dyes by semiconductor metal oxides is based on advanced oxidation process (AOP). This method is based on the creation of radicals and reactive oxygen species on absorption of light. Advanced oxidation processes (AOPs) is a potential technique for waste water treatment since they have large capacity to oxidize the organic pollutants.

In the present research work, sunlight-irradiated photocatalysis of doped ZnO nanoparticles was measured with respect to decolorization of methylene blue (MB). The kinetic rate constant ( $k$ ) of photocatalytic effect in MB degradation was determined from the absorbance coefficient,  $A(t)$ . Various photocatalytic degradation methods can be assessed

with different kinetic decay processes. The rate of kinetic decay depends on the concentration of the photo absorbing species. The photocatalytic degradation is governed according to the first order differential rate equation in which a linear relation is maintained between the logarithmic concentration  $[C(t)]$  vs. time  $t$ . The rate equation appears as

$$\frac{d[C(t)]}{dt} = -k[C(t)] \quad (2.1)$$

Where,  $k$  is the mentioned rate constant with unit of  $s^{-1}$ . On integrating this equation, we have obtained

$$\ln \frac{[C(t)]}{[C(0)]} = -kt \quad (2.2)$$

$[C(0)]$  is the initial concentration.

Conferring with Beer Lambert law the absorbance  $[A(t)]$  and concentration of the absorbing species  $[C(t)]$  maintain proportional relation. The absorbance  $[A(t)]$  is defined as

$$[A(t)] = -\log_{10} T(t) = -\log_{10} \frac{I(t)}{I_0} \quad (2.3)$$

Where,  $T(t)$  is the transmittance of the absorbing material at time  $t$ ,  $I_0$  is the intensity of initial ( $t = 0$ ) transmitted light through the solvent and container,  $I(t)$  is the intensity of transmitted light at time  $t$ , preserving the same power of light source.

Conferring with Beer Lambert law, absorbed light intensity ( $dI_z$ ) is stated through the relation as presented in figure 2.9.

$$dI_z = -I_z \sigma N dz \quad (2.4)$$

Where,  $dz$  is the width along the direction of the light,  $\sigma$  is cross-sectional area,  $N$  is the number of particles per unit volume ( $cm^3$ ). On integrating the equation over the total length ( $b$ ) towards incident light through the solution, the above relation becomes as:

$$\ln \frac{I}{I_0} = -\sigma N b \quad (2.5)$$

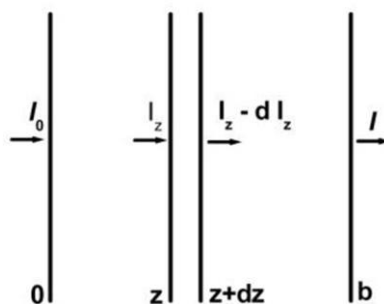


**Fig. 2.9.** Photo degradation over length.

The absorbance thus can be described as:

$$A = -\log_{10} \frac{I}{I_0} = \varepsilon[C]b \quad (2.6)$$

Where,  $\varepsilon$  is the molar absorbance and is stated through the relation  $\varepsilon = \frac{\sigma}{2.303} \left( \frac{N_0}{1000} \right)$ ,  $N_0$  is

the Avogadro number and  $[C]$  is the molar concentration of the absorbing materials. The relation exhibits that the absorbance  $A(t)$  is directly proportional to the molar concentration  $[C(t)]$  at time  $t$ . As such Eq. (2.2) can be modified using absorbance as

$$\ln \frac{[C(t)]}{[C(0)]} = \ln \frac{[A(t)]}{[A(0)]} = -kt \quad (2.7)$$

Eq. (2.7) denote that the rate constant,  $k$  can be acquired from the slope of the curve

$\ln \frac{[A(0)]}{[A(t)]}$  vs. time, which follows the first order rate law for the photocatalytic degradation.

### 2.2.6. Electrical characterization:

Dielectric properties of pure and doped ZnO nanocompounds have been investigated by LCR 3522-50 LCR Hi TESTER (HIOKI, Japan). In the frequencies ranges of 100 Hz to 100 kHz the dielectric constant is a contribution of the polarization mechanisms such as electronic, ionic, dipolar and interfacial polarization present in the sample. Some of the dipolar modes cease with increasing frequency and in result the dielectric constant decreases.

The ferroelectric property of nanoparticle samples has been observed using digital oscilloscope and laboratory made Sawyer-Tower (S-T) circuit. Sawyer and Tower first

proposed a circuit to obtain the ferroelectric hysteresis nature on the oscilloscope [183]. We have adopted this circuit with slight modification and able to record all the parameters linked with hysteresis loop with variation of electric field amplitude at room temperature [184].

The electrical characterizations of the sample have been done after calcinations of the prepared nanopowders at required temperatures for the different doped ZnO compounds. The calcined materials were finally compressed into pellets and the pellets were sintered at essential temperature and time. The flat faces of the pellet were coated with silver to form the electrodes.

#### **2.2.7. Magnetic characterization (SQUID magnetometer):**

SQUID is being used to analyze the magnetic properties of compounds from very low to very high magnetic fields. In this device, an external magnetic field of 0-10 Tesla is employed to the sample by a strong superconducting magnet. The specimen is made to pass gradually through a set of pickup coils coupled with superconducting wires. The output voltage recognized through SQUID magnetometer and the corresponding magnetic moment of the material maintain a proportional relation. SQUID magnetometer operates according to superconducting Josephson junctions and is very sensitive to any small variation in magnetic flux. The measurement of the sample can be made at the temperature range from liquid helium (5K) to room temperature and also with the variation of magnetic field at fixed temperature. In this present research work the magnetic hysteresis curve of prepared samples has been investigated through SQUID magnetometer at 5K with the magnetic field of  $\pm 4$  tesla.

#### **2.2.8. ME characterization:**

For ME measurement the sample was exposed to poling for ordering the electric and magnetic dipoles using electrical and magnetic field respectively [185]. ME coupling at

room temperature has been investigated using a ME set-up (Marine India) linked to a lock-in-amplifier. The electrical poling at 0.98 kV/cm for 12 hr and the magnetic poling at 5 kOe for 1 hr were conducted for ME measurement. The ME coefficient was measured using dynamic method in which both the magnetic field AC and DC was applied [186]. The voltage produced from the sample was measured using ME set-up linked with a lock-in-amplifier when the sample was set aside in longitudinal mode. Experimentally, AC magnetic fields with 1 kHz frequency and 15.37 Oe magnitude was applied with a varying DC magnetic field of magnitude (-5 kOe to 5 kOe). The AC magnetic field was developed by a Helmholtz coil with the parameters  $N = 200$  turns, radius  $r = 2.5$  cm and coil resistance  $R = 23.4 \Omega$  connected with a function generator. The AC magnetic field with magnitude  $h_0$  produced at the center of the Helmholtz coil can be determined from the expression:

$$h_0 = \frac{\mu_0}{4\pi} \frac{2\pi N I r^2}{\left(r^2 + \frac{r^2}{4}\right)^{\frac{3}{2}}} \times 2 = \frac{\mu_0}{\left(\frac{5}{4}\right)^{\frac{3}{2}}} \frac{N I}{r} = 8.99 \times 10^{-3} \times \frac{N V}{r R} \text{ Oe} \quad (2.8)$$

In this set up, 5 V AC was fed to the Helmholtz coil and in result 15.37 Oe magnetic field was obtained. The application of the magnetic field ( $H$ ) through the sample produces an induced electric field ( $E$ ) across the faces of the sample. The relation of these two fields appears as [187]:

$$E = \frac{V}{d} = f(H) = \text{Constant} + \alpha H + \beta H^2 + \gamma H^3 + \dots \quad (2.9)$$

$$\Rightarrow \frac{dE}{dH} = \alpha + 2\beta H + 3\gamma H^2 + 4\delta H^3 + \dots \quad (2.10)$$

The total magnetic field can be expressed as:  $H_{total} = H + h_0 \sin \omega t$ . The ME voltage coefficient,  $\alpha_E$  is calculated using the relation [188, 189]

$$\alpha_E = \left( \frac{dE}{dH} \right)_{H=0} \quad (2.11)$$